Organic Geochemistry 195 (2024) 104810

Contents lists available at ScienceDirect

Organic Geochemistry

journal homepage: www.elsevier.com/locate/orggeochem

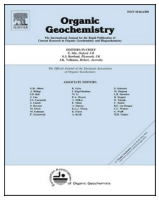

Investigating the application of organic geochemical techniques to tropical Anjohibe (Madagascar) stalagmites

Robin R. Dawson [a,*], Isla S. Castañeda [a], Stephen J. Burns [a], Jeffrey M. Salacup [a], Nick Scroxton [b], David McGee [c], Peterson Faina [d], Laurie R. Godfrey [e], Lovasoa Ranivoharimanana [f]

[a] Department of Earth, Geographic and Climate Sciences, 233 Morrill Science Center, 627 North Pleasant Street, University of Massachusetts Amherst, Amherst MA 01003-9297, USA
[b] Irish Climate and Analysis Research Units, Department of Geography, Laraghbryan House, Maynooth University, Co. Kildare, Ireland
[c] Department of Earth, Atmospheric and Planetary Sciences, Massachusetts Institute of Technology, 77 Massachusetts Avenue, Cambridge, MA 02139, USA
[d] The Climate School, Columbia University, New York, NY 10025, USA
[e] Department of Anthropology, 219 Machmer Hall, University of Massachusetts, Amherst, MA 01003, USA
[f] Mention Bassins sédimentaires, Evolution, Conservation, Faculté des Sciences, Université d'Antananarivo, Antananarivo, Madagascar

ARTICLE INFO

Associate Editor — Rienk Smittenberg

Keywords:
Stalagmites
Plant waxes
Polycyclic aromatic hydrocarbons
Compound specific stable isotope analysis
Land-use change

ABSTRACT

Speleothem stable carbon isotopes ($\delta^{13}C_{carb}$) are used to reconstruct past environments, but are a complex signal of karst, soil and plant processes. To help untangle these signals, we used plant waxes, their carbon isotopic values ($\delta^{13}C_{wax}$) and polycyclic aromatic hydrocarbons (PAHs) extracted from stalagmites to evaluate plant photosynthetic pathway (C_3 vs C_4) and biomass burning above a cave. Our test case investigates stalagmites from Anjohibe in Madagascar where at around 1000 CE multiple $\delta^{13}C_{carb}$ records increase by ~ 8–10 ‰. This suggests that humans transformed the local landscape from C_3 vegetation to C_4 grasses through agropastoral practices, which rely on burning to promote grass growth. We evaluated different protocols to remove contamination, finding higher biomarker yields after polishing off the surface of the stalagmite versus ultrasonic pre-cleaning in solvent. Anjohibe stalagmites include *n*-alkanes from trees and grasses; however, bulk organic $\delta^{13}C$ and $\delta^{13}C_{wax}$ from samples dated to after the transition to the modern C_4 landscape yield values suggesting C_3 vegetation. This is likely due to a disproportionally higher contribution of C_3 waxes to the overall *n*-alkane signal. PAHs are present in the stalagmite but do not match the types found in overlying soils and further testing is required to determine their source. We find that $\delta^{13}C$ values of bulk organic carbon, or plant waxes extracted from stalagmites, should be interpreted with caution as the proportion of plant matter on the landscape does not necessarily equate to the proportion of organic molecules produced by those plants or preserved in the sedimentary record.

1. Introduction

Speleothems have long provided a wealth of information for understanding terrestrial paleoclimate (Hendy and Wilson, 1968), especially after improved precision in U-Th dating techniques (Shen et al., 2002). Their mineralogy, trace metal and stable isotope chemistry document past changes in the monsoons, occurrences of droughts and other changes in paleo-hydrology (Bar-Matthews et al., 2003; Medina-Elizalde et al., 2010; Wang et al., 2001). The most commonly used climate proxies in speleothems are the stable carbon ($\delta^{13}C$) and oxygen ($\delta^{18}O$) isotopes of carbonate. The former is thought to reflect carbon input to karst systems from the atmosphere, soil and vegetation above the cave (Wong and Breecker, 2015), while the latter primarily reflects the isotopic value of precipitation (McDermott et al., 2005). Of the two, $\delta^{18}O$ is the more easily explained within a climate framework, with variability reflecting changes in rain amount, moisture source, and temperature (Fairchild et al., 2006). Variability in $\delta^{13}C$ in speleothem carbonate is more difficult to interpret and is far less often used as an environmental proxy because a wide variety of processes may influence the signal, including: vegetation type, soil processes related to moisture and temperature, prior calcite and aragonite precipitation, disequilibrium reactions in the karst, changes in the partial pressure of carbon dioxide (pCO_2) in the cave atmosphere and degree of degassing of cave drip waters (Fohlmeister et al., 2020). Because of these complexities,

* Corresponding author.
E-mail address: rrdawson@umass.edu (R.R. Dawson).

https://doi.org/10.1016/j.orggeochem.2024.104810
Received 11 March 2024; Received in revised form 26 May 2024; Accepted 27 May 2024
Available online 28 May 2024

$\delta^{13}C$ records have often been ignored or unreported in speleothem-based climate studies. Recently, combined $\delta^{13}C$ and trace element (Mg/Ca, Sr/Ca) measurements have been used to explore and even quantify the role of hydrology (mainly prior carbonate precipitation) on speleothem $\delta^{13}C$ (Stoll et al., 2023). Paired $\delta^{13}C$ and ^{14}C measurements are revealing the role of differently aged organic matter (OM) sources in speleothem $\delta^{13}C$ (Lechleitner et al., 2016). However, the role of changing vegetation remains relatively unexplored.

Biomarkers can be described as molecular fossils and include compounds or classes of compounds preserved in the rock record that can be traced to specific organisms, group of organisms or biological reactions (e.g. photosynthesis) (Castañeda and Schouten, 2011; Killops and Killops, 2005). They have the potential to directly identify vegetation changes in speleothems, and therefore the role of those vegetation changes on speleothem $\delta^{13}C$. Blyth and others have investigated whether speleothems contain more direct information about vegetation and climate in the organic carbon compounds found in low concentrations in speleothems (Blyth et al., 2007; Blyth et al., 2006; Blyth et al., 2013a; Blyth et al., 2013b) and (Li et al., 2014; Wang et al., 2019). If this organic component can be extracted, its geochemistry (e.g. plant wax biomarkers and $\delta^{13}C$ values of individual compounds) might be used to directly identify vegetation changes using well-dated speleothems. These studies have outlined techniques to extract bulk organic carbon $\delta^{13}C$ (Blyth et al., 2013a; Blyth et al., 2013b; Li et al., 2014), specific organic compounds such as plant waxes (e.g. *n*-alkanes, fatty acids; Blyth et al., 2006; Wang et al., 2019) and other compound classes such as archeal membrane lipids (Blyth and Schouten, 2013) as well as to measure their stable isotopic compositions (Blyth et al., 2013b; Wang et al., 2019). In studies of Heshang Cave, China, Wang and others (2019) argue for evidence of more C_3 vegetation and soil respiration in the early Holocene based on compound specific $\delta^{13}C$ of different chain lengths of fatty acids, whereas no change is recorded by the inorganic $\delta^{13}C$ from the same sample (Hu et al., 2008). Other researchers have measured and quantified polycyclic aromatic hydrocarbons (PAHs) in speleothems, which are molecular indicators of biomass burning and fire but can also be derived from petrogenic sources (Argiriadis et al., 2019; Argiriadis et al., 2024; Perrette et al., 2008). Preliminary work on speleothems from lava tubes in the Galápagos has also found biomarkers indicative of anthropogenic stress on the environment (Miller et al., 2022). Despite methodological advancements including acid digestion, liquid–liquid phase separation (LLPS) (e.g. Blyth et al., 2006) and clean lab protocols (e.g., Argiriadis et al., 2019), a major challenge with this work is the very low concentration of organic carbon (0.01–0.3 % total carbon) in cave deposits (Blyth et al., 2016). Additionally, like other paleoenvironmental archives (e.g., lake sediments, peats), questions remain regarding the source, transport and preservation of organic compounds in speleothems.

In this study we test whether these organic molecular tools can be applied to detect a well-established vegetation turnover approximately 1,000 years ago in northwestern Madagascar. Here, an ecosystem shift from a dry deciduous forest ecosystem dominated by flora using a C_3 photosynthetic pathway to a grassy biome dominated by C_4 grasses was likely caused by human activity and involved, in part or in full, the introduction of slash and burn agriculture (Burns et al., 2016; Godfrey et al., 2019). Evidence for this shift is recorded by a large increase in grass pollen in lakes across Madagascar (Burney, 1987; Gasse and Van Campo, 1998; Matsumoto and Burney, 1994; Teixeira et al., 2021), and is seen in speleothems from Anjohibe ('big cave' in Malagasy) via a large, ~10 ‰ positive excursion in carbonate $\delta^{13}C$ (hereafter $\delta^{13}C_{carb}$) (Burns et al., 2016; Voarintsoa et al., 2017). Thus, we consider speleothems from Anjohibe, in comparison to above-cave soil and plant samples, to be an ideal test case to determine whether various organic biomarkers are present in speleothems, whether they record information on the overlying soil and vegetation, and whether they can detect ecosystem scale changes in overlying vegetation. If the organic material contained in speleothems is reflective of surface processes, then the large shift in $\delta^{13}C_{carb}$ should also be recorded in one or more organic compounds held in the same speleothems.

2. Material and methods

2.1. Study site and field sampling

Anjohibe is located about 70 km northeast of Mahajanga (−15.542° latitude, 46.885° longitude) and formed in the Eocene Narinda Limestone (Besairie, 1972; Middleton and Middleton, 2002), with overlying bedrock thickness ranging from 1 to 10 m below the land surface (Voarintsoa et al., 2021). Today, the environment above the cave is primarily savanna C_4 grasses with scattered palms and small C_3 trees (Supplementary Fig. 1) in wetter areas such as at cave entrances (Voarintsoa et al., 2021).

We tested organic geochemical methods on three speleothems (AB2, AB3 and AB4) collected in 2014. The $\delta^{13}C_{carb}$ of AB2 and AB3 has been previously published (Burns et al., 2016; Scroxton et al., 2017) and includes the distinctive ~ 10 ‰ enrichment at ~ 1 ka marking the transition from predominantly C_3 to C_4 vegetation. Stalagmite AB4 was never analyzed in detail for carbonate isotopes due to very large uncertainties of the U/Th ages, with a top age of 3554 ± 1664 years BP (Before Present) and a bottom age of 5796 ± 6391 years BP. Based on these two ages, any geochemical information recorded in sample AB4 should reflect the paleoenvironment prior to the recorded ecosystem shift. In other words, it should reflect a C_3-dominated deciduous forest landscape. Prior to destructively sampling material from the well dated AB2 and AB3 stalagmites, AB4 was used for testing extraction methods because it contained ample amounts of carbonate that could be dissolved for biomarker analysis. Soil and plant samples above Anjohibe and nearby Anjohikely ('little cave', −15.561° latitude, 46.874° longitude) were also collected in October 2019 to test as possible sources of biomarkers found in the speleothem samples.

2.2. Speleothem OM

2.2.1. Controlling for modern OM contamination on speleothems

A summary of the chemistry workflow for the stalagmite sample preparation is shown in Fig. 1. Because the OM content of speleothems is very low, contamination of sample surfaces during sample collection, handling and preparation is a serious concern. Previous studies of OM in speleothems have removed potentially contaminated surface material by either physical or acid removal of the surface (e.g., Blyth et al., 2006; Blyth and Schouten, 2013; Blyth et al., 2013a; Wang et al., 2019) or by sampling a fragment from the speleothem and ultrasonic pre-cleaning it whole in solvent, usually dichloromethane (DCM) or 9:1 DCM: methanol (MeOH) (e.g., Argiriadis et al., 2019; Blyth et al., 2007). However, the stalagmites from Anjohibe can be quite porous, reflecting a mixture of calcite and aragonite layers and ultrasonic pre-cleaning is likely unable to differentiate between removing contaminant organic molecules on the surface of the fragment versus paleo-molecules within the layers of the stalagmite. Therefore, we tested two methods of removing contamination.

The first method is based on previously published methods (e.g. Argiriadis et al., 2019; Blyth et al., 2007) and involved ultrasonic pre-cleaning a portion of the stalagmite in solvent. We used either a ~ 2 cm diamond-tipped coring drill bit to obtain cylinders of stalagmite carbonate or a diamond tile saw to cut chips of stalagmite along the growth axis. These fragments were then sonicated in 9:1 DCM:MeOH either 5× for 3 min (Blyth et al., 2007) or 3× for 15 min. Since previous studies used a range of different weights (~200 mg to 10 g), we also tested the ultrasonic pre-cleaning protocol on samples between 1–13 g. An in-house marble standard was powdered and combusted at 500 °C to eliminate all OM and used as a check standard for the organic geochemistry protocol described below.

The second method to remove surface contamination is newly

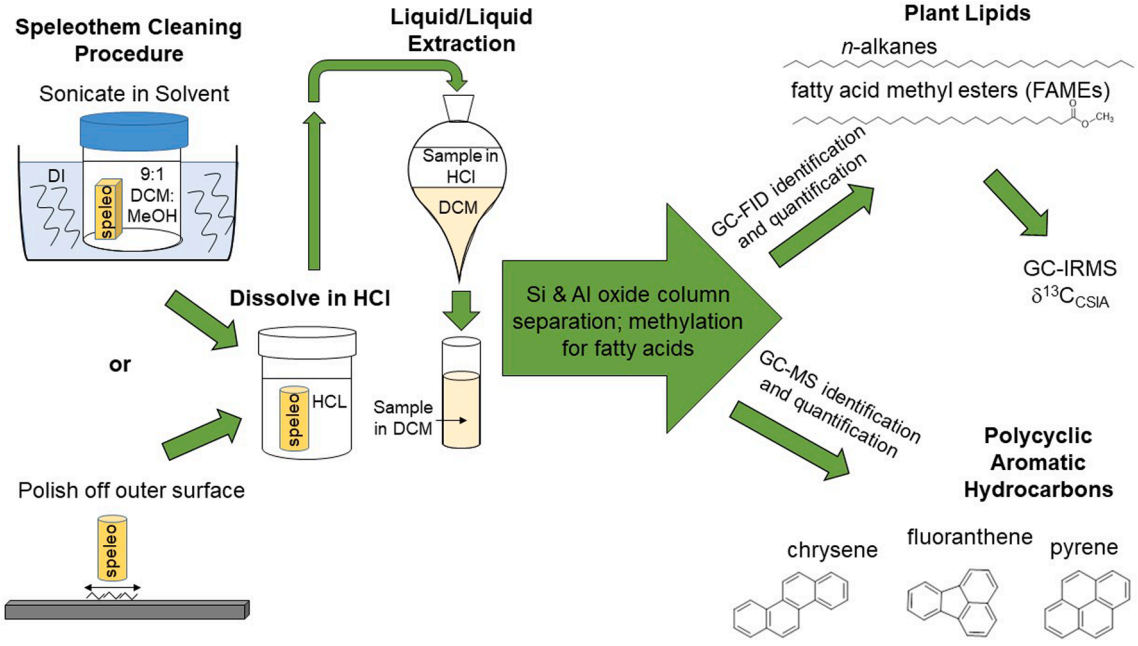

Fig. 1. Schematic of organic geochemistry workflow.

proposed here and involves physical removal, using a diamond encrusted metal polishing plate. Polishing grit, paste or pads used in standard thin-sectioning practices were not used to avoid OM contamination. Subsamples of stalagmite were drilled at different depths along the growth axis using a ~ 2 cm diamond-tipped coring drill bit to obtain cylinders of stalagmite carbonate that weighed between 9–12 g. The outside surfaces of the carbonate cylinders were then polished off to remove any modern surface OM contamination. All metal tools including the polishing plate and core drill bit were rinsed prior to and between sampling using 9:1 DCM:MeOH. The same in-house marble was also sampled using the same core drill bit and polished to serve as a test of this new method to remove surface contamination.

2.2.2. Speleothem OM Extraction and Chromatography

After one of the two surface cleaning pretreatment methods was followed, stalagmite samples were dissolved in 34–37 % TraceGrade HCl pre-extracted with solvent (DCM) to remove contamination. All glassware used was cleaned and combusted in a 500 °C muffle furnace for 6 h. A solvent cleaned stir bar was added to the reaction beaker to facilitate dissolution. The beakers were covered with a petri dish during the dissolution (which usually took a couple hours to overnight) while allowing CO_2 to escape via the spout. After the stalagmite fragment was dissolved, any dissolved OM was extracted from the acid 3 times by LLPS using DCM in a separatory funnel. Subsequently the DCM fractions were combined to obtain a total lipid extract (TLE); excess solvent was evaporated on a Zymark TurboVap. There was often residual water from the HCl and this was removed by running the TLE through sodium sulfate columns. Next the TLE was separated into neutral lipids, fatty acid and phospholipid acid fractions using aminopropyl column chromatography with mobile phases of DCM:isopropanol (2:1, v/v), ethyl ether: acetic acid (96:4, v/v) and MeOH, respectively. The neutral lipids were further separated into apolar, ketone, and polar fraction using alumina oxide column chromatography with mobile phases of hexane/DCM (9:1, v/v), hexane/DCM (1:1, v/v) and DCM/MeOH (1:1, v/v). A total of 17 samples from stalagmite AB4 and 1 from AB2 were examined; biomarkers were detected in all 18 samples. Molecules of interest for this study include the *n*-alkanes and PAHs which are predominantly in the apolar fraction. For all types of samples (speleothem extract, soil, plant), apolar fractions were subsequently run through silver nitrate impregnated silica gel columns with hexane (100 %) and ethyl acetate (100 %) to separate saturated and unsaturated hydrocarbons prior to analysis on the GC-IRMS.

Fatty acids or *n*-alkanoic acids are another type of leaf wax molecule that can be extracted from sediments, although they are not as recalcitrant as *n*-alkanes (Cranwell, 1981). Questions remain about the production, isotopic fractionation, transport and preservation differences between *n*-alkanes and fatty acids in living plants (Diefendorf and Freimuth, 2017). Regardless, fatty acids may provide important environmental information, and were extracted to obtain information about the past environment above Anjohibe. The fatty acid fraction was acetylated using 5:95 acetyl chloride:MeOH and the sample vials were placed in a metal holder, on a heating block set to 60 °C and allowed to react to completion overnight. Water was then removed using LLPS with a 5 % NaCl solution and hexane. The fatty acid fraction was further cleaned using silica gel and extracted with DCM. The end products are fatty acid methyl esters or FAMEs. Plant waxes (*n*-alkanes and FAMEs) were quantified by a gas chromatograph (GC) equipped with a Flame Ionization Detector (GC-FID). PAHs were identified and quantified by GC–MS (see sections 2.4 and 2.5 for more details).

2.3. Soil and plant samples

In addition to the stalagmites, modern topsoils (n = 3; approximately 0 to 20 cm depth) and plants (n = 9) from the ground surface above Anjohibe were collected in October 2019 to compare biomarker content (plant waxes, PAHs) and $\delta^{13}C_{organic}$ of potential sources to that of the stalagmite layers. Topsoils were collected near the primary entrance to Anjohibe where small trees grow today, and near an entrance above the cave that is surrounded by grassland. A third topsoil was taken from a grassy area above Anjohikely. Plants with either C_3 or C_4 photosynthetic pathways were also collected from the surrounding area, along with an introduced non-native cactus (from a local farmer) representative of plants that use the Crassulacean Acid Metabolism (CAM). Plants were either identified in the field or classified to the family level using field notes and photos along with the Kew Royal Botanic Gardens Plants of the World Online database (POWO, 2022).

Modern topsoil samples were freeze-dried, homogenized, and extracted using a Dionex automated solvent extractor (ASE 200) with a solvent mixture of 9:1 (v/v) DCM:MeOH. Modern plant samples were extracted ultrasonically also using 9:1 (v/v) DCM:MeOH. Samples were

sonicated 3 times for 30 min and extracts combined to obtain the TLE. Both topsoil and plant TLEs followed the same aminopropyl, alumina column, and silver nitrate impregnated silica gel chromatography procedures as described above.

2.4. Plant Waxes (GC-FID)

The *n*-alkanes and FAMEs were identified and quantified on an Agilent 7890A gas chromatograph (GC) equipped with a Flame Ionization Detector (GC-FID). Samples were injected (1μl) from an autosampler into the inlet (splitless, 250 °C) and carried via hydrogen gas (flow rate of 4.5 ml min^{-1}) onto a 60m DB-5 column (0.32 mm ID, 0.25 μm film). The oven temperature initiated at 70 °C, increased at a rate of 17 °C min^{-1} to 130 °C, and next at 7 °C $min^{-1}$to 320 °C; the final temperature of 320°C was held for 15 min. Concentrations of each compound were determined using a calibration curve of the standard squalane, which was injected at 8 concentrations ranging from 2 to 75 ng/μL. To assess sample recovery after each step (e.g. acid dissolution and column chromatography), a known concentration of a standard (squalane) was also added to the sample beaker prior to dissolution. Recovery of plant waxes was 84 % efficient after acid dissolution, and between 53–77 % efficient after acid dissolution and column chromatography.

2.5. Polycyclic Aromatic Hydrocarbons (GC–MS)

For the speleothem and soil samples, PAHs within the apolar fraction were identified and quantified on a Hewlett Packard 6890 series GC coupled to an Agilent 5973N mass spectrometer (GC–MS) with a Restek Rtx-5 ms column (60 m × 250 μm × 0.25 μm). The oven temperature initiated at 70 °C, increased at a rate of 20 °C min^{-1} to 130 °C, and next at a rate of 4 °C min^{-1} to 320 °C; the final temperature of 320 °C was held for 20 min. Samples were analyzed in Selected Ion Monitoring (SIM) mode, where ion masses of 17 PAHs were targeted. PAH concentrations were calculated using an external calibration curve based on varying concentrations of a mixture of 16 PAHs from a RESTEK SV Calibration Mix combined with Retene from a CHIRON AS standard. See methods in Miller et al. (2017) for more details.

2.6. Plant Wax $\delta^{13}C$ (GC-IRMS)

Plant waxes (*n*-alkanes and FAMEs) were targeted for compound specific isotope analysis (CSIA) if specific chain lengths of interest were found in high enough concentrations (at least ~ 60 ng/μl for our instrument) to obtain reliable carbon isotope measurements. If concentrations were sufficient, sample $\delta^{13}C_{wax}$ (*n*-alkanes or FAMEs) was measured on a Thermo Delta V Advantage Isotope Ratio Mass Spectrometer (IRMS) coupled to a Thermo Trace GC Ultra through a GCC III or a Thermo Trace 1310 through an IsoLink II. Samples were injected (4μl) from an autosampler into a 280 °C inlet (splitless) and onto a DB-1 MS column (30 m, 0.25 mm ID, 0.25 μm film). The oven temperature initiated at 70 °C, increased at a rate of 25 °C min^{-1} to 230 °C, and next at a rate of 5 °C min^{-1} to 320 °C; the final temperature of 320°C was held for 10 min. Helium was used as a carrier gas at a flow rate of 1.2 ml min^{-1}. The oxidation and reactor temperatures were 940 °C and 650 °C respectively on the GCC III. On the IsoLink II the reduction furnace was set at 1000 °C. When we had enough material samples were run in duplicate and normalized to Vienna Pee Dee Belemnite (VPDB) using an external standard (*n*C28#2, Arndt Schimmellmann, Indiana University). Precision and accuracy were tracked via comparison with a standard of known value (*n*C25#4, Arndt Schimmelmann, Indiana University). Deviation in accuracy of our reconstructed $\delta^{13}C$ was 0.0 +/- 0.2 ‰. Precision, measured using the average of repeat measurements, was +/- 0.2 ‰.

2.7. Total lipid extracts/TLEs (EA-IRMS)

In addition to CSIA, some samples of stalagmites and plants were analyzed for the $\delta^{13}C$ of bulk extracted OM ($\delta^{13}C_{TLE}$). For these analyses, a few drops of the TLE were added to a pre-weighed tin capsule, the solvent allowed to evaporate fully, and subsequently weighed. These samples were analyzed at the Yale Analytical and Stable Isotope Center (YASIC) on a Costech ECS 4010 Elemental Analyzer with Conflo III interface for isotope ratios on an IRMS. The in-house reference materials run at Yale are standardized to the Vienna Peedee Belemnite (VPDB) and give a standard deviation of at least 0.2 ‰.

2.8. Ratios to describe OM

N-alkane data is often summarized using the average chain length (ACL), which is the weighted average of the various carbon-chain lengths (Bush and McInerney, 2013) and is defined as:

$$ACL = \frac{\sum(C_n \times n)}{\sum(C_n)}$$

C_n is the concentration of each *n*-alkane with *n* carbon atoms. This and other chain-length ratios are often thought to be indicative of different plant functional groups. For example, the ratio of C_{29}/C_{31} or $C_{31}/(C_{31} + C_{29})$ has been used to try and differentiate savannah versus rainforest habitats (Jansen et al., 2008; Vogts et al., 2009), though this might be more reflective of climate than an actual difference between grass and woody plant types (Bush and McInerney, 2013). Another common ratio used to examine *n*-alkanes in paleorecords is the carbon preference index (CPI) (Marzi et al., 1993). This describes the odd- over even-carbon number predominance and is defined as:

$$CPI = \frac{[\sum_{odd}(C_{21-33}) + \sum_{odd}(C_{23-35})]}{[2\sum_{even}(C_{22-34})]}$$

CPI values vary greatly in modern plants (Bush and McInerney, 2013), but it is commonly reported that a CPI > 1 indicates immature (not thermally altered) plant matter.

3. Results and discussion

3.1. Recovery of plant waxes from stalagmites

The two different methods for removing surface contaminants from stalagmite samples showed highly variable yields of plant waxes (C_{28} FAMES and C_{29} *n*-alkanes) (Fig. 2). These chain-lengths are abundant in both grasses and woody plants (Bush and McInerney, 2013) and so were chosen as a target molecule for assessing $\delta^{13}C$ CSIA potential of these stalagmite samples. As expected, the combusted marble standard did not contain any *n*-alkanes. For the smaller AB4 samples (~1 g) that were sonicated clean, yields were between 7–13 ng C_{29} *n*-alkanes. These amounts are well below the ~ 60 ng of C_{29} *n*-alkanes required for CSIA on our GC-IRMS. A previous study of an Australian stalagmite (Argiriadis et al., 2019) yielded ~ 1000–2000 ng C_{29} *n*-alkanes g^{-1} carbonate, though the authors see a lack of odd-over-even preference suggesting a source other than plants for these lipids. Another previous study on a speleothem from Ethiopia (Blyth et al., 2006) showed lower yields between ~ 60–100 ng g^{-1} carbonate for C_{31} *n*-alkanes and C_{28} *n*-alkanols, with the authors acid digesting ~ 10 g of stalagmite carbonate per sample. The lower leaf wax yields in AB4 could be due to lower primary productivity above Anjohibe than the other two caves or slower and less fracture flow of OM to the stalagmite surface. Lower concentrations of plant waxes make careful laboratory preparation and instrument precision essential when working in this type of setting. It is important to use internal standards to test sample recovery as well as carbonate standards such as marble to identify any possible sources of contamination.

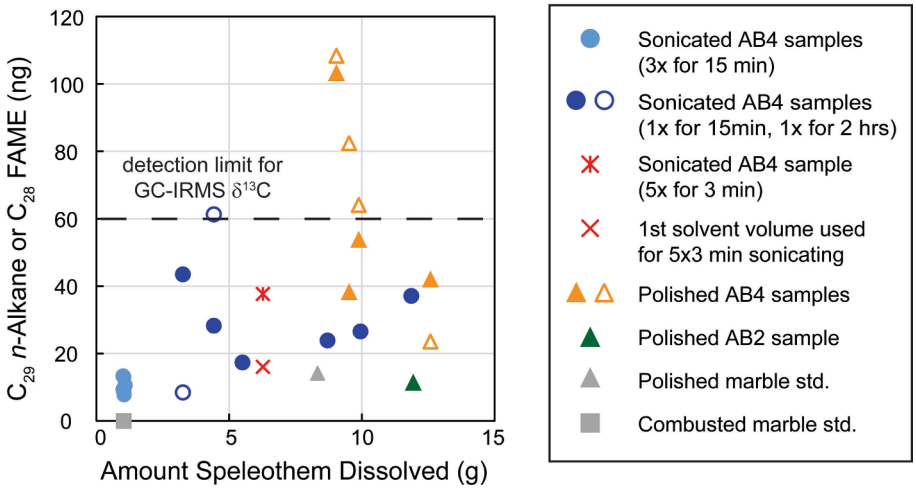

Fig. 2. Total amount (ng) of C_{29} *n*-alkanes (filled symbols) and C_{28} FAMEs (open symbols) extracted from stalagmite sample AB4 using two different methods for removing surface contamination and C_{29} *n*-alkanes from stalagmite AB2 sample and marble standards.

Since 1 g of speleothem AB4 did not provide enough material for CSIA, it was subsequently resampled by drilling 3–12 g of speleothem. Interestingly, there is no 1:1 relationship between the amount of speleothem carbonate dissolved and the yield of extracted plant waxes, with values ranging from 17 to 44 ng for C_{29} *n*-alkanes and 8–63 ng C_{28} FAMES (Fig. 2). Though this set of six AB4 samples was sonicated for a longer period during the second sonication step (close to 2 h), compared to the 6 samples weighing ~ 1 g each, they show no evidence of excessive loss of organic molecules due to the extra sonication time. Although there was no predictable increase in organic molecules with increased carbonate dissolved, we decided to dissolve close to 10 g of AB4 going forward to have a better chance of reaching the 60 ng detection limit for CSIA. To examine how much plant wax was removed after ultrasonic pre-cleaning, we saved the solvent used for ultrasonic cleaning another sample of AB4 (red X in Fig. 2) and compared it to the quantity of waxes eventually extracted from the carbonate after acid dissolution (red X with a vertical line in Fig. 2). For this sample, we sonicated it 5× for 3 min in 9:1 DCM:MeOH. The amount of C_{29} *n*-alkanes (16 ng) removed and presumed to be contamination from the first sonication is about the same as the amount extracted post acid dissolution from another sample with similar mass (~6 g) sonicated for 15 min and then 2 h (17ng). This emphasizes that the sample signal is very small and on the scale of possible contamination.

Ultimately there is no way to determine whether the lipids removed during sonication are sample or contamination. The AB4 speleothem is quite porous and therefore the solvent used for ultrasonic cleaning likely reacts with OM not only on the cut outer surface of the speleothem, but also within these pore spaces, where primary OM was deposited at the time the speleothem layers were formed. Therefore, with none of the ultrasonically cleaned samples except one yielding enough plant waxes (C_{28} FAMES) for CSIA, we instead turned to the polishing method of removing contaminated stalagmite surfaces in hopes of extracting higher yields of primary organic molecules.

Four samples of AB4, polished on each side to remove contamination, ranged in mass from 9 to 13 g and the amount of extracted plant waxes ranged from 38 to 103 ng for C_{29} *n*-alkanes and 24–108 ng C_{28} FAMES (Fig. 2). On average, this method recovered more plant waxes than ultrasonic cleaning, but again, there is no linear relationship between the amounts of carbonate dissolved and extracted plant waxes. We explored how much organic contamination might be on the tools used, including the polishing plate used to remove surface contamination and the drill bit used to sample AB4. Therefore, we saved both the solvent (9:1 DCM:MeOH) used to clean the tools prior to sampling and polishing and the solvent used to clean the tools again before the next sample. These "pre-cleaning" and "post-cleaning" solvent rinses were treated as samples and run through the chromatography steps to compare with AB4. The full range of potential plant wax compounds of interest were present as contamination on these tools (Fig. 3). We concluded that it is essential to pre-clean the polishing plate and drill bit prior to sampling. These findings support previous work on Archean drill cores (French et al., 2015), which found that initial sampling with inadequately cleaned saw blades was a major source of biomarker contamination. Likewise, it is important to clean tools with solvent between sampling to remove any residual OM from the previous sample (Fig. 3).

When comparing the solvent washes (Fig. 3) to the AB4 sample that was acid digested and extracted by LLPS (Fig. 3), we see that in contrast to the potential contamination rinsed off the sampling tools, the waxes extracted from a clean sample of AB4 exhibit the classic odd-over-even predominance expected from plant waxes. However, the solvents used for cleaning the tools have a smoother distribution of all chain lengths (Fig. 3) and a low CPI (1.01–1.03). The CPI values for *n*-alkanes from the 4 polished samples from stalagmite AB4 and one polished sample from AB2 range from 1.40 to 1.82, suggesting a source from terrestrial higher plants (Fig. 4). The CPI range of all the sonicated clean samples is 0.57 to 2.02, with most above one, again suggesting a biological source. The polished marble standard CPI is 0.89, while the combusted marble standard CPI is 0.22. One AB4 sample extracted from ~ 1 g of carbonate had a very low CPI (0.57), within the range of the marble standards. This sample also had the lowest yield of total *n*-alkanes between C_{21}-C_{40} (97 ng). This is a reminder that any interpretation from *n*-alkane ratios should be made with caution when working with samples with such low organic molecule yields.

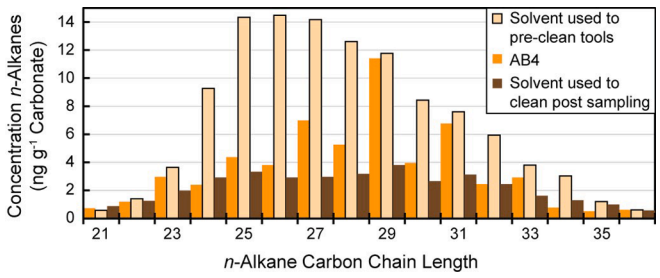

Fig. 3. Concentration of *n*-alkanes from solvent used to pre-clean the drill bit and polishing plate used to sample stalagmite material from AB4, extracted AB4 stalagmite (RRD 39), and solvent used to clean the same drill bit and polishing plate before next sample.

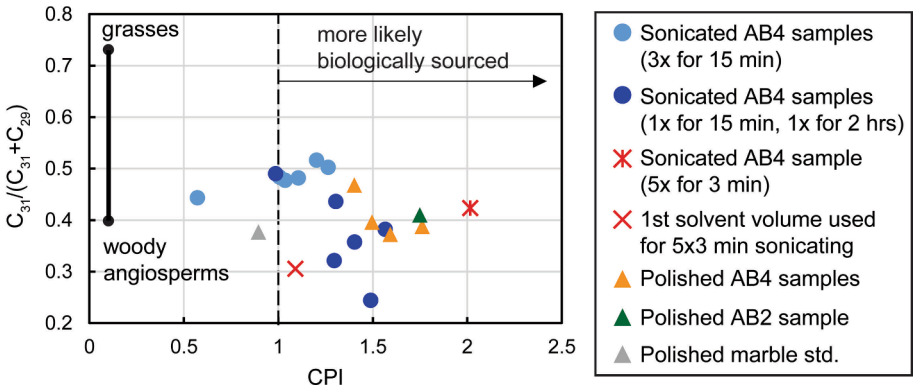

Fig. 4. Carbon preference index (CPI) versus the n-alkane chain length ratio $C_{31}/(C_{31} + C_{29})$ for all stalagmite samples and marble standard. The dashed line at a CPI value of 1 differentiates alkanes derived from higher plant sources from those derived from degraded or mature organic matter. The solid black line on the left side of the plot shows endmember values of the $C_{31}/(C_{31} + C_{29})$ ratio for woody angiosperms and grasses (based on Bush and McInerney, 2013).

The ACL of all polished speleothem samples ranged from 26.7 to 28.3 while the ACL of all sonicated AB4 samples included some longer chain lengths and ranged from 26.6 to 30.2. The first solvent rinse saved from extracting AB4 (5 x for 3 min) had *n*-alkanes in it with an ACL of 25.1, while ultimately the carbonate dissolved and extracted after that 5x3 minute sonication cleaning protocol, yielded *n*-alkanes with an ACL of 26.9. They also differed in CPI, with the solvent rinse being 1.09 and the sample 2.02 (Fig. 4). All leaf wax data from testing different stalagmite extraction methods and marble standards are listed in Supplementary Tables 1 and 2 (*n*-alkanes) and Supplementary Table3 (FAMES).

3.2. Comparison of plant waxes from Anjohibe 3 ka and ~ 600 ya

Since concentrations of plant waxes in the Anjohibe samples were rarely high enough to analyze $\delta^{13}C_{wax}$, we explored using *n*-alkane chain length ratios such as $C_{31}/(C_{31} + C_{29})$ to estimate relative inputs from woody angiosperms versus grasses through time. Ratios of C_{31} and C_{29} *n*-alkanes have been proposed by previous studies (Jansen et al., 2008; Vogts et al., 2009), to reflect the transition from forests to grasslands, with forests producing more of the shorter C_{29} chain length. However these chain length differences might also reflect wetter (shorter chain lengths) versus drier (longer chain lengths) climates (Bush and McInerney, 2013). The 4 polished AB4 samples were drilled at roughly equally-spaced depths throughout the ~ 2 m length of the stalagmite. Geochemical data they provide reflect vegetation at ~ 3 ka, and we can compare these 4 samples to the sample taken from AB2 at ~ 295–315 mm, which reflects the environment ~ 600 years ago, after the shift to a savanna ecosystem (Scroxton et al., 2017). Modern African grasses produce *n*-alkane chain length ratios of $C_{31}/(C_{31} + C_{29})$ averaging 0.731, while woody angiosperms have an average value of 0.399 (Bush and McInerney, 2013). Interestingly, we find that the $C_{31}/(C_{31} + C_{29})$ value for AB4 samples (0.373–0.468) and the AB2 sample (0.410) are similar (Fig. 4), though the latter grew after the landscape above Anjohibe became C_4-dominated. It is unlikely the ~ 10 ‰ increase in $\delta^{13}C_{carb}$ at 1000 CE reflects a mere replacement of C_3 grasses by C_4 grasses with no change in the relative abundance of C_3 trees. C_3 grasses are found in shaded forest or mosaic landscapes and at elevations above 2000 m and C_4 grasses do not thrive in shady habitats (Silander et al., 2024). The change from C_3 to C_4 was far more rapid (~100 years) than expected for climate driven fluctuations, and there is no correlation between carbon and oxygen isotope values at the time of the habitat shift, as would be expected if the change were triggered by climate. This supports the idea that it was caused instead by human agropastoralist practices (Burns et al., 2016; Godfrey et al., 2019). A loss of C_3 trees near Anjohibe at ~ 1000 CE is also strongly supported by subfossil data showing the local extirpation of endemic large-bodied arboreal taxa with C_3 plant diets after 1500 years ago, as well as the fact that introduced species (including rats and shrews, as well as domesticated animals), had largely C_4 diets (Crowley and Samonds, 2013). The lack of expected signal in the $C_{31}/(C_{31} + C_{29})$ value could be due to other factors, such as temperature or aridity, which can influence *n*-alkane chain-length or because chain-length distributions are not an exact indicator of plant type. It is also possible our AB2 sample never received surface *n*-alkanes produced after the landscape changed. Uncertainties remain about the transport and lag time between various carbon reservoirs for *n*-alkanes from plant to speleothem.

We can also compare the overall concentrations of *n*-alkanes extracted from these samples that represent the older more C_3 dominated landscape (AB4) and the younger C_4 dominated landscape (AB2). The total C_{21}-C_{40} *n*-alkane yields averaged 312 ng for the polished AB4 samples, while the AB2 sample total yields averaged only 74 ng, which is less than that detected in the polished marble standard (130 ng). These differences are obvious when normalized to grams carbonate dissolved per extraction (Fig. 5). In addition to making it difficult to interpret *n*-alkane distributions, the low concentration of *n*-alkanes in AB2 precluded $\delta^{13}C_{wax}$ measurement. All leaf wax data from samples drilled from stalagmites AB4 and AB2 are listed in Supplementary Table 1 and 2 (*n*-alkanes) and Supplementary Table 3 (FAMES).

3.3. Plant waxes from modern plants and soils

The nine modern plants collected from the field near Anjohibe represent six families that are C_3 photosynthesizers, two families that are C_4, and one that uses CAM. The C_3 plants have the highest total concentrations of C_{21}-C_{40} *n*-alkanes, ranging from 65 to 562 μg g^{-1}, whereas the C_4 and CAM plants have 66–144 μg g^{-1}. A similar relationship is present in the total *n*-alkane concentrations extracted from the three soils collected near Anjohibe and Anjohikely. The two soils collected in a more open grass covered area had total *n*-alkane concentrations ranging

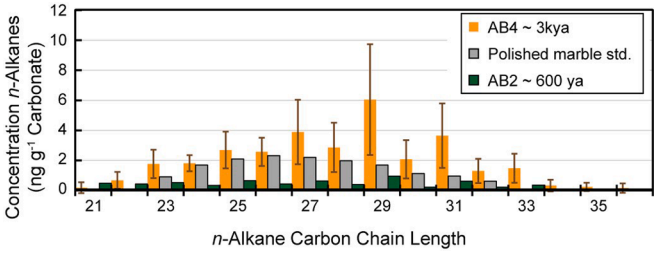

Fig. 5. Concentration of *n*-alkanes in polished stalagmite samples from AB4 (n = 4) and AB2 (n = 1) compared with a polished marble standard. AB4 bars reflect the average of 4 samples and errors bars are the standard deviation while AB2 bars reflect a single sample.

from 1 to 2 μg g^{-1} while the soil sample collected near the entrance of Anjohibe with more trees had a total concentration of 9 μg g^{-1}. The ACL of the C_3 plants analyzed here is 31.0–31.9, while the C_4 grasses is lower at 30.3–30.7 and the CAM plant is 30.2. The ACL of the two more grassy/open soils are 29.4 and 28.7, while the more tree covered Anjohibe soils is 30.6. The greater range with lower ACLs (~27–30) seen in the speleothem samples compared to the modern plants and soils could be due to the breaking of longer plant derived chains and production of shorter-chained n-alkanes by microbes in situ and en route to the speleothem surface.

Comparing different chain length distributions such as C_{31}, C_{29}, and C_{27} from the plants and soils collected near Anjohibe to the database of African plants in Bush and McInerney (2013), shows that there is overlap between C_3, C_4 and CAM plants and the chain lengths of plant waxes they produce (Fig. 6). The average $C_{31}/(C_{31} + C_{29})$ value (0.760 ± 0.079) of the modern C_3 plants collected near Anjohibe (n = 6) are actually closer to the end member for grasses (0.731) reported from the larger dataset from Bush and McInerney (2013). Likewise, the average $C_{31}/(C_{31} + C_{29})$ value (0.593 ± 0.047) for the modern C_4 grasses collected near Anjohibe (n = 2) is more towards the end member for woody angiosperms (0.399) depicted in Fig. 4. Therefore, *n*-alkane chain length distributions are not always a reliable indicator of plant type and the patterns observed with a larger dataset such as by Bush and McInerney (2013) may not be observable within specific regions represented by a smaller subset of plants. In fact, there is no significant difference in *n*-alkane distributions from samples from the ~ 3 ka AB4 stalagmite versus the ~ 600 ya AB2 stalagmite (Fig. 6), despite the latter growing after the major shift to a C_4 dominated landscape (Burns et al., 2016; Godfrey et al., 2019; Scroxton et al., 2017). The average $C_{31}/(C_{31} + C_{29})$ value for the AB4 stalagmite samples (0.406 ± 0.043) is also within error of the value for the AB2 stalagmite sample and both are closer to the value of the two modern C_4 grasses versus the modern C_3 plants collected near Anjohibe. *N*-alkane distributions appear not to be distinctive enough to differentiate plant types in this ecoregion. All *n*-alkane data from modern plants and soils collected near Anjohibe and the nearby Anjohikely are provided in Supplementary Tables 4 and 5.

3.4. Polycyclic aromatic hydrocarbons from soils and stalagmites

Low molecular weight (LMW) PAHs (e.g. phenanthrene, anthracene, fluoranthene, pyrene, retene) compared to high molecular weight (HMW) PAHs (e.g. Benzo(a)anthracene, Chrysene, Benzo(b)fluorenthene, Benzo(k)fluorenthene, Benzo(a)pyrene, Indeno(1,2,3-cd) pyrene) are useful in differentiating burned plant types with potential applications in the sedimentary record (Karp et al., 2020). In our three soil samples we find LMW PAHs including fluoranthene, pyrene, and retene in concentrations from 3.9 to 17.2 ng g sed^{-1} (Fig. 7). We also detect 16.3 ng g sed^{-1} of a high molecular weight (HMW) PAH, dibenz(a,b)anthracene. Though we found no notable differences in either concentration or types of PAHs between the more C_3 plant-covered versus C_4 plant-covered modern-day soils (Fig. 7). No PAHs were detected in the sample of stalagmite AB2 (grew ~ 600 ya), despite its deposition after the transition to a C_4 vegetated landscape due to agropastoral burning. The PAHs extracted from stalagmite AB4 samples (grew ~ 3 ka) most reflect HMW PAHs (*m/z* above 228) with only one sample containing the LMW PAHs (e.g. fluoranthene and pyrene) found in the modern soils (Fig. 7). Concentrations of PAHs from the polished AB4 samples range from 0.3 to 2 ng g^{-1} stalagmite, which is an order of magnitude lower than the concentrations found in the soils (Fig. 7). The ultrasonic pre-cleaned AB4 samples had higher concentrations of PAHs from 0.8 to 7.9 ng g^{-1} stalagmite. This could be due to chance and the location on the stalagmite from which the sample was drilled or due to contamination. These concentrations are within the range found in previous studies (Argiriadis et al., 2019; 2024) of stalagmites from northwestern Australia that track historical records of fire. Although the Australian cave and Anjohibe are located in similar environments, PAH proxy work may be more difficult at Anjohibe, because of its larger size and thus more complicated or slower infiltration pathways for PAHs. Slower growing stalagmites at Anjohibe may also contribute to the lack of PAHs in AB2 samples. Another study by Perrette et al. (2008) on material from France found higher concentrations of LMW PAHs in stalagmite samples (~20–30 ng g^{-1}) but lower concentrations overall in soils, including LMW PAHs (~1–12 ng g^{-1}), suggesting that the PAHs in the stalagmite reflect a "reservoir effect". It is clear from the overall lack of similarity between the stalagmites of Anjohibe and nearby soils that the stalagmite PAHs warrant further study. Without this, these PAHs cannot be used as reliable paleoenvironmental indicators.

We extracted PAHs from the solvent used to clean the polishing plate and drill bit after sampling and cleaning an AB4 sample (RRD 39). The concentrations and PAH types are similar to those extracted from the AB4 samples themselves (Fig. 7), indicating the post solvent wash does remove PAHs from the sampling tools and could be helpful in preventing

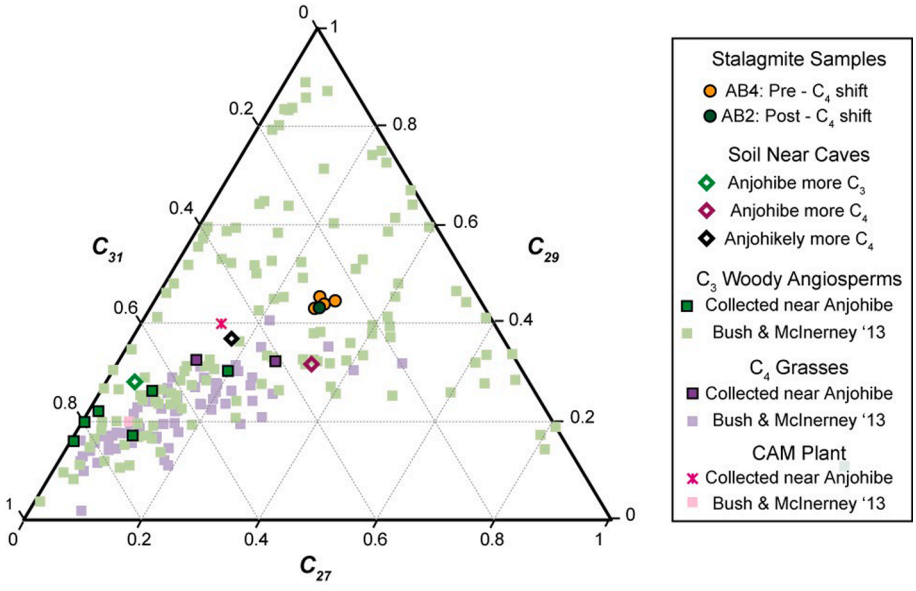

Fig. 6. Ternary diagram comparing different chain lengths of n-alkanes extracted from plants, soils and Anjohibe stalagmites. Previously published data of African plants compiled in Bush and McInerney, (2013) and Vogts et al., (2009) are also plotted.

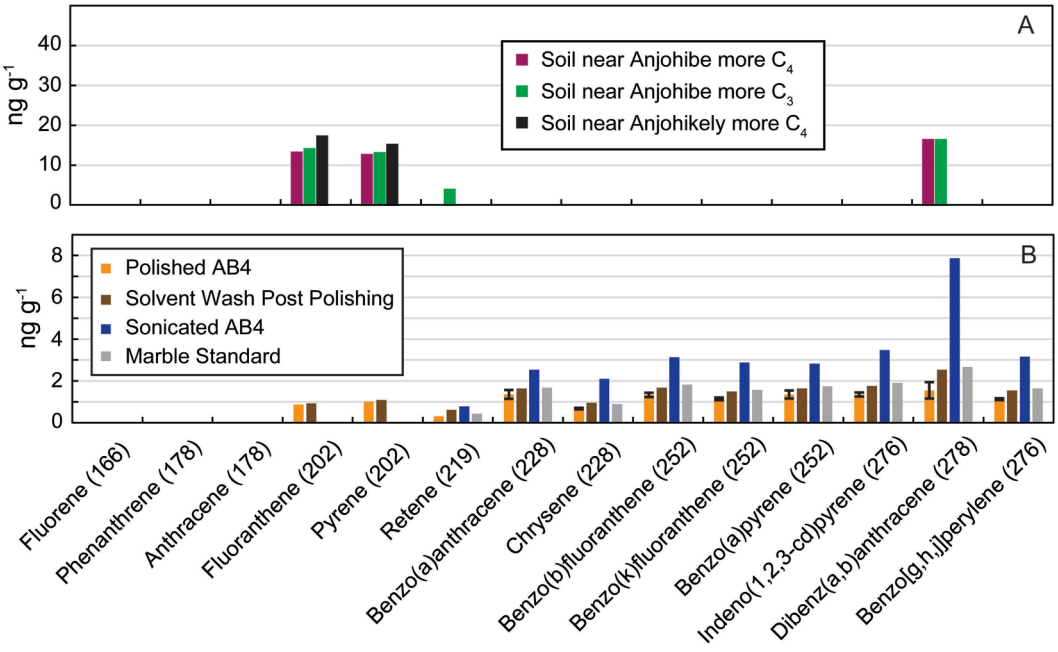

Fig. 7. PAH concentrations (ng/g) in soils (A) and AB4 stalagmite samples (B). *m/z* associated with each PAH shown on x-axis. Polished AB4 average values are shown with standard deviation error bars.

sample cross-contamination. However we also found similar concentrations of PAHs in the marble standard, suggesting a PAH source from contamination throughout the chemical workup. A previous study by (Argiriadis et al., 2019), sonicated the piece of stalagmite before acid dissolution and extraction, and tested recovery of PAHs using a known amount of the compounds added to 0.5g of Carrara marble. They found PAH recovery between 90 and 163 %, also suggesting some additional sources of PAHs were incorporated into the Carrara marble extract via contamination at steps in the laboratory protocol. At such low sample concentrations, contamination can heavily skew interpretations. Therefore, questions remain as to the source of PAHs in stalagmite samples, and we conclude that PAHs are not reliable paleoenvironmental signals in this case. All of our PAH concentrations are given in Supplementary Table 6.

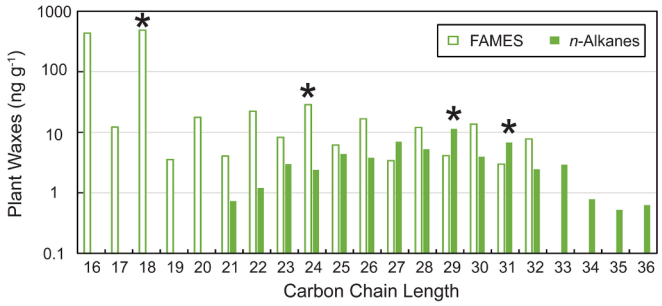

Fig. 8. Concentration of FAMES and *n*-alkanes in a polished stalagmite sample from AB4. Chain lengths marked with an asterisk were measured for CSIA. Note the logarithmic scale on the y-axis.

3.5. Compound specific stable isotopes ($\delta^{13}C_{wax}$) from Anjohibe

We obtained enough plant waxes in one AB4 sample to analyze $\delta^{13}C_{wax}$ of the C_{29} (11 ng g^{-1}) and C_{31} (7 ng g^{-1}) *n*-alkanes, chosen because they are commonly produced by woody angiosperms and grasses (Bush and McInerney, 2013; Vogts et al., 2009). The $\delta^{13}C_{wax}$ (VPDB) values for these chain lengths are –32.3 ‰ and –33.7 ‰ respectively. Like previous studies (Blyth et al., 2011; Wang et al., 2019; Xie et al., 2003) we found a bimodal distribution of chain lengths for our FAMES, with the highest abundances in the shorter chain lengths (C_{16} and C_{18}) which are represented in all biomass including bacteria and plants. The next most abundant chain length, C_{24}, is attributed to plant waxes (Fig. 8). Therefore, we analyzed the $\delta^{13}C_{FAMES}$ of C_{18} and C_{24} chain lengths, following a previous study which used these values to estimate changes in soil respiration (Wang et al., 2001). We extracted enough FAMES (>10 ng g^{-1}) in three AB4 samples (including the same one analyzed for $\delta^{13}C_{wax}$) to run CSIA. The average $\delta^{13}C_{FAME}$ values and standard deviations of C_{18} and C_{24} are 30.4 ± 0.6 ‰ and –32.4 ± 0.5 ‰, respectively.

The $\delta^{13}C$ values of the long-chain waxes (C_{29}, C_{31}, C_{24}) from AB4 overlap with published $\delta^{13}C_{wax}$ values from modern C_3 plants (Chikaraishi et al., 2004; Vogts et al., 2009) (Fig. 9). Modern C_3 plants (n = 5) collected near Anjohibe have C_{31} *n*-alkanes $\delta^{13}C$ values with a mean and standard deviation of −39.5 ± 3.9 ‰, whereas modern collected C_4 and CAM plants (n = 3) have C_{31} *n*-alkanes $\delta^{13}C$ values averaging −20.8 ± 1.1 ‰ (Fig. 9). A modern soil collected near the main entrance to Anjohibe, where trees are present, gives a C_{31} *n*-alkane $\delta^{13}C$ value of −35.8 ‰. Unfortunately, the soil collected near an Anjohibe entrance surrounded by grassland did not produce enough material for CSIA. However, a soil from Anjohikely, surrounded by grassland, albeit with a *Pachypodium* tree growing nearby, gave a C_{31} *n*-alkane $\delta^{13}C$ value of −30.1 ‰. These modern $\delta^{13}C_{wax}$ values from samples collected near Anjohibe are also plotted in Fig. 9 and show that the longer chain length $\delta^{13}C_{wax}$ values from AB4 are close to the C_{31} *n*-alkane $\delta^{13}C$ value of modern C_3 plants and C_3 dominated soils versus the modern C_4 plants. The AB4 $\delta^{13}C_{wax}$ values are representative of OM from ~ 3 ka, and thus support the theory that prior to ~ 1 ka, C_3 plants dominated the landscape above Anjohibe. The C_{18} FAME $\delta^{13}C$ values are higher and likely sourced from both plants and bacteria (Xie et al., 2003), and do not overlap with the modern C_3 plants (Fig. 9). All CSIA data is listed in Supplementary Table 7.

3.6. Bulk organic carbon (TLE) stable isotopes from Anjohibe

Because we did not recover enough plant waxes after extracting ~ 12

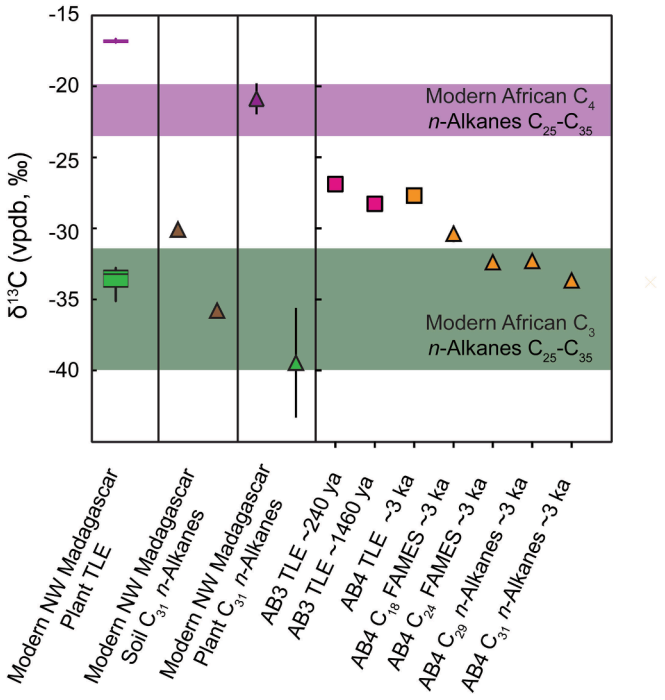

Fig. 9. Compound specific (triangles) and TLE (boxes) $\delta^{13}C$ values from Anjohibe stalagmite samples AB4 (orange) and AB3 (pink) and TLE $\delta^{13}C$ values from modern C_3 (green) and C_4 (purple) plants collected near Anjohibe, Madagascar. Error bars are standard deviation. The green and purple boxes represent the wide range of $\delta^{13}C$ values seen in plant waxes of other modern C_3 and C_4 plants respectively (Vogts et al., 2009).

g of the well-dated sample AB2, two samples from AB3 were extracted, also previously published in Burns et al. (2016). We sampled AB3 at 50 mm and 700 mm, which based on the previously published age model (Burns et al., 2016), should contain OM that represents ~ 1,460 years before present (prior to the shift to a C_4 dominated landscape) and ~ 240 years before present (after the shift to a C_4 dominated landscape). These samples were extracted and then the TLEs put into tin capsules and weighted to measure $\delta^{13}C_{TLE}$. The younger AB3 sample yielded a $\delta^{13}C_{TLE}$ value of −26.9 ‰ and the older AB3 sample a $\delta^{13}C_{TLE}$ value of −28.3 ‰ (Fig. 9). Thus, these samples follow the expected trend given the known vegetation shift on the landscape although the difference in values is fairly small.

Overall, less TLE was recovered per gram of dry plant for the C_4 and CAM plants (6–18 mg g^{-1}) compared to C_3 plants (8–76 mg g^{-1}). The three soil samples had no obvious differences and TLEs ranged from 1.3 to 1.7 mg g^{-1}. Although there is no obvious distinction in dominant plant wax chain lengths among C_3 and C_4 plant types from near Anjohibe, there is an offset in their bulk $\delta^{13}C$ due to their different methods of CO_2 fixation (O'Leary, 1988). The average $\delta^{13}C_{TLE}$ of all C_3 plants is –33.6 ± 1.17 ‰ while the average $\delta^{13}C_{TLE}$ of the C_4 grasses is −16.8 ± 0.17 ‰. Comparing the modern Madagascar plant $\delta^{13}C_{TLE}$ values to both the AB3 and AB4 Stalagmite $\delta^{13}C_{TLE}$ values, the stalagmite values fall between the modern Anjohibe C_3 and C_4 plant $\delta^{13}C_{TLE}$ values (Fig. 9) and close to the average for C_3 plant matter (−28 ‰) reported in (O'Leary, 1988). All bulk organic carbon (TLE) isotope data is listed in Supplementary Table 8.

Previous work (O'Leary, 1988) and the C_4 samples collected near Anjohibe, suggest that the younger AB3 sample should have a $\delta^{13}C_{TLE}$ value in the range of −14 ‰ to −17 ‰ (Fig. 9).

We attribute the lack of $\delta^{13}C$ offset between the younger and older samples to the large difference in concentrations of plant waxes produced by the different plant types. The C_3 plants near Anjohibe produced three times more C_{21}-C_{40} *n*-alkanes (median concentration 210 μg g^{-1}) than the C_4 and CAM plants (median concentration 81 μg g^{-1}). A global compilation of *n*-alkane data (Bush and McInerney, 2013) shows that C_3 plants generally produce less total *n*-alkanes (median concentration 107 μg g^{-1}) than C_4/CAM plants (median concentration 458 μg g^{-1}). However, the range of *n*-alkane concentrations for C_3 plants is much larger than C_4/CAM with a higher maximum concentration of 3607 μg g^{-1} compared to 1377 μg g^{-1} for C_4/CAM plants. It is therefore plausible that although the ecosystem around Anjohibe shifted from C_3 to C_4 dominated plants, the expected isotopic shift in soil and speleothem C_{org} is greatly attenuated in this region by the relatively low concentrations of *n*-alkanes in the grasses.

Based on field observations in the area around Anjohibe today, grasses cover 80–90 % of the landscape. In addition, a survey of the vegetation of Madagascar by the United Kingdom: Royal Botanic Gardens found that at least 65 % of all uncultivated land in Madagascar is covered by grasses (Moat and Smith, 2007). The concentrations of *n*-alkanes from our modern plant samples (total 1880 μg g^{-1} dry plant) can be used to estimate what proportion of *n*-alkanes comes from C_4 plants (291 μg g^{-1} dry plant). Based on this approximation, C_4 plants contribute ~ 15 % of the total *n*-alkanes delivered to the sediment record, despite being the dominant plant type in the region today. We suggest that $\delta^{13}C$ values either from bulk organic carbon or specific compounds extracted from stalagmites should be interpreted with caution as the proportion of plant matter on the landscape, and preserved in stalagmites, does not necessarily equate to the proportion of organic molecules produced by those plants.

Assuming the TLE derives entirely from higher plants, a simple two-end member mixing model, using values −34 ‰ for C_3 plants and −17 ‰ for C_4 plants (the mean modern plant $\delta^{13}C_{TLE}$ values from Fig. 9), can be used to estimate possible $\delta^{13}C_{TLE}$ values of a hypothetical stalagmite based on what proportion of the landscape is either C_3 or C_4.

$$\delta^{13}C_{stal-TLE} = [F_{C_3}(\delta^{13}C_{C_3})] + [F_{C_4}(\delta^{13}C_{C_4})]$$

$$F_{C_3} + F_{C_4} = 1$$

If we estimate that 80 % of the organic carbon in the stalagmite TLE is from C_4 plants, then our hypothetical stalagmite $\delta^{13}C_{TLE}$ value would be −20 ‰. This is higher than the $\delta^{13}C_{TLE}$ value measured in the AB3 sample dated to 240 years ago ($\delta^{13}C_{TLE}$ value of −27 ‰) at which point C_4 plants dominate. It's possible that our observed $\delta^{13}C_{TLE}$ value is more negative than expected due to, as discussed above, less overall C_4 plant waxes delivered to the soil. Another possibility is that soil microbial contributions could influence $\delta^{13}C_{TLE}$ values and obscure the vegetation change. Therefore, it is important when interpreting $\delta^{13}C$ records from organic carbon, whether compound specific or bulk, to consider not only the relative proportion of plant type on the landscape, but also how different plant types produce different amounts of organic carbon including diagnostic molecules like plant waxes and how they get into the stalagmite. A similar consideration must be made when interpreting $\delta^{13}C_{carb}$ as it has been found that cave CO_2 is mostly derived from CO_2 respired from plants with the deepest roots. These tend to be C_3 plants and their signal can dominate even if they sparsely cover the landscape (Breecker et al., 2012). In addition, microbes in the soil and vadose zone along the flow path to a stalagmite, contribute OM (allochthonous) and alter transported OM (e.g. plant waxes) on the way to the stalagmite surface where in situ microbial communities contribute their own OM (autochthonous). These various OM sources all contribute to the $\delta^{13}C_{TLE}$ value and are largely controlled by water–rock residence times and flow rates through the karst system (Blyth et al., 2016). For example, biomarkers such as leaf waxes and PAHs could reside for hundreds to thousands of years in a well-developed soil before being transported to the surface of a speleothem resulting in a lag between the organic carbon produced on the surface and that carbon being incorporated into a stalagmite. Alternatively, fast flow of organic molecules via groundwater infiltrating cracks in the karst could happen on seasonal to annual

timescales.

4. Conclusions

The goal of this study was to test existing organic geochemistry techniques commonly used in paleoclimate studies of sediments on stalagmites from northwestern Madagascar where a change in vegetation and fire history occurred ~ 1 ka (Burns et al., 2016; Godfrey et al., 2019; Scroxton et al., 2017). Our methods were based on previous work (Argiriadis et al., 2019; Blyth et al., 2016; Wang et al., 2019) and although we attempted to limit variables by testing these techniques on relatively young stalagmites with well-understood paleoclimate and fire history, we still encountered challenges that need to be considered in future studies of OM contained in speleothems. First and foremost, it is very difficult to subsample speleothems and isolate the organic compounds contained within them without introducing contamination. This difficulty is exacerbated due to the very low content of primary OM in speleothems. For our samples, we found more than 10 g of carbonate was often necessary to yield enough extracted compounds for CSIA, though other studies on cave material from more biologically productive regions might require less. Prior to attempting organic geochemistry on speleothems, we recommend exploratory sample work to determine OM concentrations. For example, previous studies confirmed that TOC is quite low in stalagmites from 0.01-0.11 ‰, based on measurements of non-purgeable OM in stalagmites (Blyth et al., 2013a; Hartland et al., 2014). Similar techniques to measure TOC could be used to screen potential stalagmite samples for organic geochemistry. In addition, questions remain as to the best ways to remove surface contamination while minimizing loss of sample.

Also, while plant waxes were recovered reliably with several methods (Argiriadis et al., 2019; Blyth et al., 2006), their ability to differentiate plant types of interest in the region around the cave should be considered to determine if the work is worthwhile. For example, longer chain length C_{27}, C_{29}, C_{31} *n*-alkanes and descriptive ratios such as ACL and $C_{31}/(C_{31} + C_{29})$ do not reliably differentiate grasses and woody plants (Bush and McInerney, 2013) and did not show any change across the C_3/C_4 ecosystem transition at Anjohibe (Fig. 6; Supplementary Table 1). Similarly, we did not see any large change in $\delta^{13}C_{TLE}$ across this transition despite a ~ 10 ‰ increase in the $\delta^{13}C_{carb}$ (Burns et al., 2016; Scroxton et al., 2017). This lack of signal in the organics is likely due to a lower amount of both total extractable lipids (median TLE 9.7 mg/g) and *n*-alkanes (median value 73.4 mg/g) produced by C_4 grasses as compared to C_3 vegetation (23.5 mg/g and 210.3 mg/g respectively). Although we cannot know for certain how much of the original plant lipid pool is preserved in the geologic record, unequal contribution of OM to the sedimentary record might also explain why the younger AB2 sample which likely grew when C_4 plants dominated, produced an order of magnitude fewer *n*-alkanes than the samples from the older AB4, which formed when C_3 plants dominated (Fig. 5). Therefore, comparing modern local plant and soil samples to stalagmite results is essential when attempting organic geochemistry techniques on a new cave record. Another possible explanation for the discrepancy between the large negative $\delta^{13}C_{carb}$ and small $\delta^{13}C_{TLE}$ signals before and after the C_3 to C_4 transition, could be different turnover rates in the initial carbon sources. The $\delta^{13}C_{carb}$ signal is determined by the DIC in the overlying soil and bedrock, which likely responds rapidly to a change in overlying vegetation. In contrast, the $\delta^{13}C_{TLE}$ signal is determined by the OM produced by plants, which could reside for much longer in the soil before being transported to the surface of the stalagmite.

Our stalagmite samples contained very low concentrations of LMW PAHs, while HMW PAHs were an order of magnitude lower than detected in our soils (Fig. 7). These differences and the absence of any PAHs in sample AB2, which grew during a known time of human burning of the landscape, suggest that there is still much to learn regarding the transport mechanisms of PAHs to stalagmites and the residence time of PAHs in the soil near Anjohibe. Recovery of PAHs in marble standards from this study (Fig. 7) and Argiriadis et al. (2019) suggests contamination. This highlights the importance of careful sample preparation and caution when interpreting results where sample PAH yields are as high as the marble contamination. Future work on young cave deposits and surrounding soils with historically documented fire history could help answer remaining questions around the transport processes and reservoir effect of PAHs in stalagmites and could help us tease apart possible sources of PAHs from the environment or contamination. In summary, while the potential for organic geochemistry proxies on well dated speleothems is exciting, more work is necessary to determine whether a given cave setting is likely to yield organic geochemical records that add information about local plant communities and fire frequency.

Data availability

All data reported in this manuscript is available in the main text and supplementary materials.

CRediT authorship contribution statement

Robin R. Dawson: Writing – review & editing, Writing – original draft, Visualization, Methodology, Formal analysis. **Isla S. Castañeda:** Writing – review & editing, Supervision, Resources, Methodology. **Stephen J. Burns:** Writing – review & editing, Resources, Project administration, Funding acquisition, Conceptualization. **Jeffrey M. Salacup:** Writing – review & editing, Validation, Methodology. **Nick Scroxton:** Writing – review & editing, Resources. **David McGee:** Writing – review & editing, Resources. **Peterson Faina:** Writing – review & editing, Resources. **Laurie R. Godfrey:** Writing – review & editing, Resources. **Lovasoa Ranivoharimanana:** Writing – review & editing, Resources.

Declaration of competing interest

The authors declare that they have no known competing financial interests or personal relationships that could have appeared to influence the work reported in this paper.

Acknowledgements

This research was conducted under a collaborative accord between the University of Massachusetts Amherst (Department of Anthropology, Department of Earth, Geographic and Climate Sciences) and Université d'Antananarivo, Madagascar (Bassins sédimentaires, Evolution, Conservation). We thank the Ministry of Higher Education and Scientific Research, the Ministry of Mines and Strategic Resources, and Ministry of Communication and Culture for permission to conduct research in Madagascar. This research made use of the Yale Analytical and Stable Isotope Center at Yale University. We thank Brad Erkkila for assistance with the EA-IRMS analyses done at YASIC. This work was supported by the National Science Foundation awards AGS-2102923/2102975, and AGS-1702891/1702691 to SJB and DM and BCS 1750598 to LRG and SJB. The authors would like to thank Richard Vachula and an anonymous reviewer for their time and effort in providing thoughtful comments that helped improve the manuscript.

Appendix A. Supplementary material

Supplementary data to this article can be found online at https://doi.org/10.1016/j.orggeochem.2024.104810.

References

Argiriadis, E., Denniston, R.F., Barbante, C., 2019. Improved polycyclic aromatic hydrocarbon and *n*-alkane determination in speleothems through cleanroom sample processing. Analytical Chemistry 91, 7007–7011.

Argiriadis, E., Denniston, R.F., Ondei, S., Bowman, D.M.J.S., Genuzio, G., Nguyen, H.Q. A., Thompson, J., Baltieri, M., Azenon, J., Cugley, J., Woods, D., Humphreys, W.F., Barbante, C., 2024. Polycyclic aromatic hydrocarbons in tropical Australian stalagmites: a framework for reconstructing paleofire activity. Geochimica et Cosmochimica Acta 366, 250–266.

Bar-Matthews, M., Ayalon, A., Gilmour, M., Matthews, A., Hawkesworth, C.J., 2003. Sea-land oxygen isotopic relationships from planktonic foraminifera and speleothems in the Eastern Mediterranean region and their implication for paleorainfall during interglacial intervals. Geochimica et Cosmochimica Acta 67, 3181–3199.

Besairie, H., 1972. Géologie de Madagascar. I. Les terrains sédimentaires. Annales Geologiques De Madagascar. 35, 1–463.

Blyth, A.J., Farrimond, P., Jones, M., 2006. An optimised method for the extraction and analysis of lipid biomarkers from stalagmites. Organic Geochemistry 37, 882–890.

Blyth, A.J., Asrat, A., Baker, A., Gulliver, P., Leng, M.J., Genty, D., 2007. A new approach to detecting vegetation and land-use change using high-resolution lipid biomarker records in stalagmites. Quaternary Research 68, 314–324.

Blyth, A.J., Baker, A., Thomas, L.E., Van Calsteren, P., 2011. A 2000-year lipid biomarker record preserved in a stalagmite from north-west Scotland. Journal of Quaternary Science 26, 326–334.

Blyth, A.J., Hartland, A., Baker, A., 2016. Organic proxies in speleothems - New developments, advantages and limitations. Quaternary Science Reviews 149, 1–17.

Blyth, A.J., Schouten, S., 2013. Calibrating the glycerol dialkyl glycerol tetraether temperature signal in speleothems. Geochimica et Cosmochimica Acta 109, 312–328.

Blyth, A.J., Shutova, Y., Smith, C., 2013a. $\delta^{13}C$ analysis of bulk organic matter in speleothems using liquid chromatography–isotope ratio mass spectrometry. Organic Geochemistry 55, 22–25.

Blyth, A.J., Smith, C.I., Drysdale, R.N., 2013b. A new perspective on the $\delta^{13}C$ signal preserved in speleothems using LC-IRMS analysis of bulk organic matter and compound specific stable isotope analysis. Quaternary Science Reviews 75, 143–149.

Breecker, D.O., Payne, A.E., Quade, J., Banner, J.L., Ball, C.E., Meyer, K.W., Cowan, B.D., 2012. The sources and sinks of CO_2 in caves under mixed woodland and grassland vegetation. Geochimica et Cosmochimica Acta 96, 230–246.

Burney, D.A., 1987. Late Holocene vegetational change in central Madagascar. Quaternary Research 28, 130–143.

Burns, S.J., Godfrey, L.R., Faina, P., McGee, D., Hardt, B., Ranivoharimanana, L., Randrianasy, J., 2016. Rapid human-induced landscape transformation in Madagascar at the end of the first millennium of the Common Era. Quaternary Science Reviews 134, 92–99.

Bush, R.T., McInerney, F.A., 2013. Leaf wax *n*-alkane distributions in and across modern plants: Implications for paleoecology and chemotaxonomy. Geochimica et Cosmochimica Acta 117, 161–179.

Castañeda, I.S., Schouten, S., 2011. A review of molecular organic proxies for examining modern and ancient lacustrine environments. Quaternary Science Reviews 30, 2851–2891.

Chikaraishi, Y., Naraoka, H., Poulson, S.R., 2004. Hydrogen and carbon isotopic fractionations of lipid biosynthesis among terrestrial (C3, C4 and CAM) and aquatic plants. Phytochemistry 65, 1369–1381.

Cranwell, P.A., 1981. Diagensis of free and bound lipids in terrestrial detritus deposited in a lacustrine sediment. Organic Geochemistry 3, 79–89.

Crowley, B.E., Samonds, K.E., 2013. Stable carbon isotope values confirm a recent increase in grasslands in northwestern Madagascar. The Holocene 23, 1066–1073.

Diefendorf, A.F., Freimuth, E.J., 2017. Extracting the most from terrestrial plant-derived *n*-alkyl lipids and their carbon isotopes from the sedimentary record: A review. Organic Geochemistry 103, 1–21.

Fairchild, L.J., Frisia, S., Borsato, A., Tooth, A.F., 2006. Speleothems. In: Nash, D.J., McLaren, S.J. (Eds.), Geochemical Sediments and Landscapes. Blackwells, Oxford, pp. 200–245.

Fohlmeister, J., Voarintsoa, N.R.G., Lechleitner, F.A., Boyd, M., Brandtstätter, S., Jacobson, M.J., Oster, J.L., 2020. Main controls on the stable carbon isotope composition of speleothems. Geochimica et Cosmochimica Acta 279, 67–87.

French, K.L., Hallmann, C., Hope, J.M., Schoon, P.L., Zumberge, J.A., Hoshino, Y., Peters, C.A., George, S.C., Love, G.D., Brocks, J.J., Buick, R., Summons, R.E., 2015. Reappraisal of hydrocarbon biomarkers in Archean rocks. Proceedings of the National Academy of Sciences 112, 5915–5920.

Gasse, F., Van Campo, E., 1998. A 40,000-yr pollen and diatom record from Lake Tritrivakely, Madagascar, in the southern tropics. Quaternary Research 49, 299–311.

Godfrey, L.R., Scroxton, N., Crowley, B.E., Burns, S.J., Sutherland, M.R., Pérez, V.R., Faina, P., McGee, D., Ranivoharimanana, L., 2019. A new interpretation of Madagascar's megafaunal decline: The "Subsistence Shift Hypothesis". Journal of Human Evolution 130, 126–140.

Hartland, A., Fairchild, I.J., Müller, W., Dominguez-Villar, D., 2014. Preservation of NOM-metal complexes in a modern hyperalkaline stalagmite: Implications for speleothem trace element geochemistry. Geochimica et Cosmochimica Acta 128, 29–43.

Hendy, C.H., Wilson, A.T., 1968. Paleoclimatic data from speleothems. Nature 219, 48–51.

Hu, C., Henderson, G.M., Huang, J., Xie, S., Sun, Y., Johnson, K.R., 2008. Quantification of Holocene Asian monsoon rainfall from spatially separated cave records. Earth and Planetary Science Letters 266, 221–232.

Jansen, B., Haussmann, N.S., Tonneijck, F.H., Verstraten, J.M., de Voogt, P., 2008. Characteristic straight-chain lipid ratios as a quick method to assess past forest–páramo transitions in the Ecuadorian Andes. Palaeogeography, Palaeoclimatology, Palaeoecology 262, 129–139.

Karp, A.T., Holman, A.I., Hopper, P., Grice, K., Freeman, K.H., 2020. Fire distinguishers: Refined interpretations of polycyclic aromatic hydrocarbons for paleo-application. Geochimica et Cosmochimica Acta 289, 93–113.

Killops, S., Killops, V., 2005. Introduction to Organic Geochemistry, second ed. Blackwell Publishing Ltd., United Kingdom.

Lechleitner, F.A., Baldini, J.U.L., Breitenbach, S.F.M., Fohlmeister, J., McIntyre, C., Goswami, B., Jamieson, R.A., Voort, T.S.v.d., Prufer, K., Marwan, N., Culleton, B.J., Kennett, D.J., Asmerom, Y., Polyak, V., Eglinton, T.I., 2016. Hydrological and climatological controls on radiocarbon concentrations in a tropical stalagmite. Geochimica et Cosmochimica Acta 194, 233-252.

Li, X., Hu, C., Huang, J., Xie, S., Baker, A., 2014. A 9000-year carbon isotopic record of acid-soluble organic matter in a stalagmite from Heshang Cave, central China: Paleoclimate implications. Chemical Geology 388, 71–77.

Marzi, R., Torkelson, B.E., Olson, R.K., 1993. A revised carbon preference index. Organic Geochemistry 20, 1303–1306.

Matsumoto, K., Burney, D.A., 1994. Late Holocene environments at Lake Mitsinjo, northwestern Madagascar. The Holocene 4, 16–24.

McDermott, F., Schwarcz, H., Rowe, P.J., 2005. Isotopes in speleothems. In: Leng, M.J. (Ed.), Isotopes in Palaeoenvironmental Research. Springer, The Netherlands, pp. 185–225.

Medina-Elizalde, M., Burns, S.J., Lea, D.W., Asmerom, Y., von Gunten, L., Polyak, V., Vuille, M., Karmalkar, A., 2010. High resolution stalagmite climate record from the Yucatán Peninsula spanning the Maya terminal classic period. Earth and Planetary Science Letters 298, 255–262.

Middleton, J., Middleton, V., 2002. Karst and caves of Madagascar. Cave and Karst Science 29, 13–20.

Miller, D.R., Castañeda, I.S., Bradley, R.S., D., m.,, 2017. Local and regional wildfire activity in central Maine (USA) during the past 900 years. Journal of Paleolimnology 58, 455–466.

Miller, A.Z., Jiménez-Morillo, N.T., Coutinho, M.L., Gazquez, F., Palma, V., Sauro, F., Pereira, M.F.C., Rull, F., Toulkeridis, T., Caldeira, A.T., Forti, P., Calaforra, J.M., 2022. Organic geochemistry and mineralogy suggest anthropogenic impact in speleothem chemistry from volcanic show caves of the Galapagos. iScience 25, 10455.

Moat, J., Smith, P., 2007. Atlas of the Vegetation of Madagascar. Kew Publishing, Royal Botanic Gardens, Kew, Richmond, UK.

O'Leary, M.H., 1988. Carbon isotopes in photosynthesis: Fractionation techniques may reveal new aspects of carbon dynamics in plants. Bioscience 38, 328–336.

Perrette, Y., Poulenard, J., Saber, A.-I., Fanget, B., Guittonneau, S., Ghaleb, B., Garaudee, S., 2008. Polycyclic aromatic hydrocarbons in stalagmites: Occurrence and use for analyzing past environments. Chemical Geology 251, 67–76.

POWO, 2022. Plants of the World Online. Facilitated by the Royal Botanic Gardens, Kew, Published on the Internet; http://www.plantsoftheworldonline.org/. Last accessed 11 November 2022.

Scroxton, N., Burns, S.J., McGee, D., Hardt, B., Godfrey, L.R., Ranivoharimanana, L., Faina, P., 2017. Hemispherically in-phase precipitation variability over the last 1700 years in a Madagascar speleothem record. Quaternary Science Reviews 164, 25–36.

Shen, C.-C., Edwards, R.L., Cheng, H., Dorale, J.A., Thomas, R.B., Moran, B.S., Weinstein, S.E., Edmonds, H.N., 2002. Uranium and thorium isotopic and concentration measurements by magnetic sector inductivley coupled plasma mass specrometry. Chemical Geology 185, 165–178.

Silander Jr., J.A., Bond, W.J., Ratsirarson, J., 2024. The grassy ecosystems of Madagascar in context: Ecology, evolution, and conservation. Plants, People, Planet 6, 94–115.

Stoll, H.M., Day, C., Lechleitner, F., Kost, O., Endres, L., Sliwinski, J., Pérez-Mejías, C., Cheng, H., Scholz, D., 2023. Distinguishing the vegetation and soil component of $\delta^{13}C$ variation in speleothem records from degassing and prior calcite precipitation effects. Climate of the Past 19, 2423–2444.

Teixeira, H., Montade, V., Salmona, J., Metzger, J., Bremond, L., Kasper, T., Daut, G., Rouland, S., Ranarilalatiana, S., Rakotondravony, R., Lounès Chikhi, L., Behling, H., Radespiel, U., 2021. Past environmental changes affected lemur population dynamics prior to human impact in Madagascar. Communications Biology 4, 1084.

Voarintsoa, N.R.G., Wang, L., Railsback, L.B., Brook, G.A., Liang, F., Cheng, H., Edwards, R.L., 2017. Multiple proxy analyses of a U/Th-dated stalagmite to reconstruct paleoenvironmental changes in northwestern Madagascar between 370 CE and 1300 CE. Palaeogeography, Palaeoclimatology, Palaeoecology 469, 138–155.

Voarintsoa, N.R.G., Ratovonanahary, A.L.J., Rakotovao, A.Z.M., Bouillon, S., 2021. Understanding the linkage between regional climatology and cave geochemical parameters to calibrate speleothem proxies in Madagascar. Science of the Total Environment 784, 147181.

Vogts, A., Moossen, H., Rommerskirchen, F., Rullkötter, J., 2009. Distribution patterns and stable carbon isotopic composition of alkanes and alkan-1-ols from plant waxes of African rain forest and savanna C_3 species. Organic Geochemistry 40, 1037–1054.

Wang, C., Bendle, J.A., Greene, S.E., Griffiths, M.L., Huang, J., Moossen, H., Zhang, H., Ashley, K., Xie, S., 2019. Speleothem biomarker evidence for a negative terrestrial feedback on climate during Holocene warm periods. Earth and Planetary Science Letters 525, 115754.

Wang, Y.J., Cheng, H., Edwards, R.L., An, Z.S., Wu, J.Y., Shen, C.-C., Dorale, J.A., 2001. A high-resolution absolute-dated Late Pleistocene monsoon record from Hulu Cave, China. Science 294, 2345–2348.

Wong, C.I., Breecker, D.O., 2015. Advancements in the use of speleothems as climate archives. Quaternary Science Reviews 127, 1–18.

Xie, S., Yi, Y., Huang, J., Hu, C., Cai, Y., Collins, M., Baker, A., 2003. Lipid distribution in a subtropical southern China stalagmite as a record of soil ecosystem response to paleoclimate change. Quaternary Research 60, 340–347.